Article

Hysteresis in the Physisorption of CO and N in a Flexible Pillared Layer Nickel Cyanide

Jeffrey T. Culp, Milton R. Smith, Edward Bittner, and Bradley Bockrath

J. Am. Chem. Soc., **2008**, 130 (37), 12427-12434 • DOI: 10.1021/ja802474b • Publication Date (Web): 22 August 2008

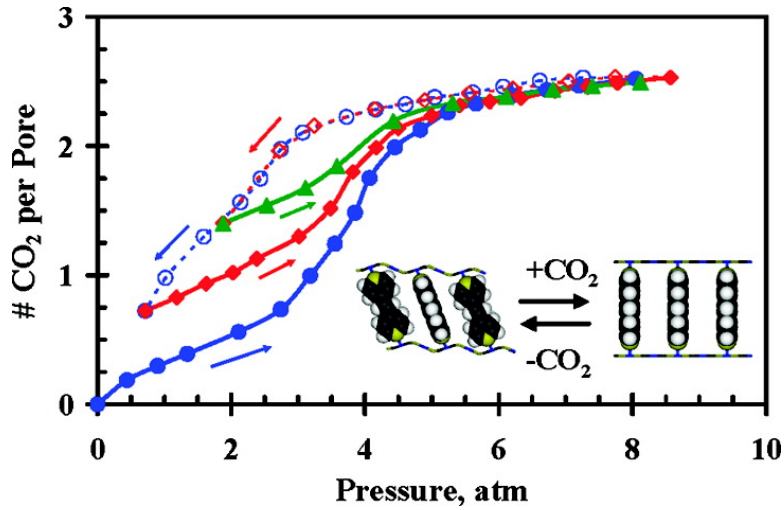

More About This Article

Additional resources and features associated with this article are available within the HTML version:

- Supporting Information
- Access to high resolution figures
- Links to articles and content related to this article
- Copyright permission to reproduce figures and/or text from this article

View the Full Text HTML

J|A|C|S
ARTICLES

Published on Web 08/22/2008

Hysteresis in the Physisorption of CO_2 and N_2 in a Flexible Pillared Layer Nickel Cyanide

Jeffrey T. Culp,*[,†,‡] Milton R. Smith,[†] Edward Bittner,[†] and Bradley Bockrath[†]

National Energy Technology Laboratory, United States Department of Energy, P.O. Box 10940, Pittsburgh, Pennsylvania 15236, and Parsons, P.O. Box 618, South Park, Pennsylvania 15129

Received April 10, 2008; E-mail: Jeffrey.Culp@pp.netl.doe.gov

Abstract: Rare hysteretic adsorption/desorption isotherms are reported for CO_2 and N_2 on a pillared Ni(1,2-bis(4-pyridyl)ethylene)[Ni(CN)$_4$] compound (NiBpeneNiCN). The hysteresis occurs under moderate pressure and at temperatures above the critical temperatures of the respective gases. Powder X-ray diffraction measurements indicate that the material is an extended three-dimensional analogue of the well-known Hofmann clathrates which is formed through axial bridging of the in-plane octahedral Ni sites by the bidentate 1,2-bis(4-pyridyl)ethylene. The hysteretic behavior toward guest adsorption and desorption is attributed to a structural phase transition in the material resulting from a variation in the tilt angle of the 1,2-bis(4-pyridyl)ethylene pillars. Kinetics studies on the desorption of acetone from the material show two first-order processes with two rate constants yielding activation energies of 68 and 55 kJ/mol when loadings are greater than 1 equiv of acetone per formula unit. The CO_2 adsorption/desorption isotherms on the series of structurally similar Ni(L)[Ni(CN)$_4$] compounds, where L = pyrazine, 4,4′-bipyridine, 1,2-bis(4-pyridyl)ethane, and dipyridylacetylene, are also reported. In contrast to NiBpeneNiCN, the rigid members of this series show normal type I isotherms with no measureable hysteresis and no significant structural changes during the adsorption/desorption cycle, while the flexible 1,2-bis(4-pyridyl)ethane-bridged sample collapses in the guest-free state and shows no significant adsorption of CO_2.

Introduction

Advances in the field of porous solids have been realized recently through the development of metal−organic frameworks (MOFs) that are flexible.[1−8] These so-called "third generation materials" are unique in their ability to undergo structural changes during the adsorption and desorption of guests.[9] The structural transition may involve a solvent-induced change from one host crystal lattice to another with an accompanying change in unit cell volume, or it may be even more pronounced where a host is regenerated from a collapsed guest-free state after re-exposure to the guest.[3,5−7,10−13]

The unique thermodynamics involved with these quasi-stable materials can greatly affect the selectivity of the adsorption process by admitting guests which are functionally matched to the pore environment, e.g., through the ability to hydrogen bond, while discriminating against guests which lack a favorable interaction.[14] As such, flexible MOFs may provide the necessary highly selective sorbents required in separation processes. In addition, the flexible nature of these hosts has led to dynamic compounds whose magnetic[15−17] or optical properties[18] change in response to a solvent stimulant. These types of signaling centers may find application in novel sensing materials.

To date, the majority of structural transformations in flexible MOFs have been observed in pseudo-one-dimensional or two-dimensional materials such as linear chain or sheet-like coordination polymers which lack an extended coordinate covalent bridge in the third dimension. The dynamic behavior of these

† National Energy Technology Laboratory.
‡ Parsons.

(1) Fletcher, A. J.; Thomas, K. M.; Rosseinsky, M. J. *J. Solid State Chem.* **2005**, *178*, 2491.
(2) Kitagawa, S.; Uemura, K. *Chem. Soc. Rev.* **2005**, *34*, 109.
(3) Kondo, A.; Noguchi, H.; Ohnishi, S.; Kajiro, H.; Tohdoh, A.; Hattori, Y.; Xu, W. C.; Tanaka, H.; Kanoh, H.; Kaneko, K. *Nano Lett.* **2006**, *6*, 2581.
(4) Serre, C.; Bourrelly, S.; Vimont, A.; Ramsahye, N. A.; Maurin, G.; Llewellyn, P. L.; Daturi, M.; Filinchuk, Y.; Leynaud, O.; Barnes, P.; Ferey, G. *Adv. Mater.* **2007**, *19*, 2246.
(5) Soldatov, D. V.; Ripmeester, J. A.; Shergina, S. I.; Sokolov, I. E.; Zanina, A. S.; Gromilov, S. A.; Dyadin, Y. A. *J. Am. Chem. Soc.* **1999**, *121*, 4179.
(6) Uemura, K.; Kitagawa, S.; Fukui, K.; Saito, K. *J. Am. Chem. Soc.* **2004**, *126*, 3817.
(7) Uemura, K.; Kitagawa, S.; Kondo, M.; Fukui, K.; Kitaura, R.; Chang, H. C.; Mizutani, T. *Chem.−Eur. J.* **2002**, *8*, 3586.
(8) Uemura, K.; Matsuda, R.; Kitagawa, S. *J. Solid State Chem.* **2005**, *178*, 2420.
(9) Kitagawa, S.; Kondo, M. *Bull. Chem. Soc. Jpn.* **1998**, *71*, 1739.
(10) Biradha, K.; Hongo, Y.; Fujita, M. *Angew. Chem., Int. Ed.* **2002**, *41*, 3395.
(11) Cussen, E. J.; Claridge, J. B.; Rosseinsky, M. J.; Kepert, C. J. *J. Am. Chem. Soc.* **2002**, *124*, 9574.
(12) Soldatov, D. V.; Enright, G. D.; Ripmeester, J. A. *Cryst. Growth Des.* **2004**, *4*, 1185.
(13) Takamizawa, S.; Nakata, E.; Yokoyama, H.; Mochizuki, K.; Mori, W. *Angew. Chem., Int. Ed.* **2003**, *42*, 4331.
(14) Kitaura, R.; Fujimoto, K.; Noro, S.; Kondo, M.; Kitagawa, S. *Angew. Chem., Int. Ed.* **2002**, *41*, 133.
(15) Halder, G. J.; Kepert, C. J.; Moubaraki, B.; Murray, K. S.; Cashion, J. D. *Science* **2002**, *298*, 1762.
(16) Maspoch, D.; Ruiz-Molina, D.; Wurst, K.; Domingo, N.; Cavallini, M.; Biscarini, F.; Tejada, J.; Rovira, C.; Veciana, J. *Nat. Mater.* **2003**, *2*, 190.
(17) Quesada, M.; de la Pena-O'Shea, V. A.; Aromi, G.; Geremia, S.; Massera, C.; Roubeau, O.; Gamez, P.; Reedijk, J. *Adv. Mater.* **2007**, *19*, 1397.
(18) Wadas, T. J.; Wang, Q. M.; Kim, Y. J.; Flaschenreim, C.; Blanton, T. N.; Eisenberg, R. *J. Am. Chem. Soc.* **2004**, *126*, 16841.

Scheme 1. Pillared Layered Ni(L)[Ni(CN)$_4$] Compounds

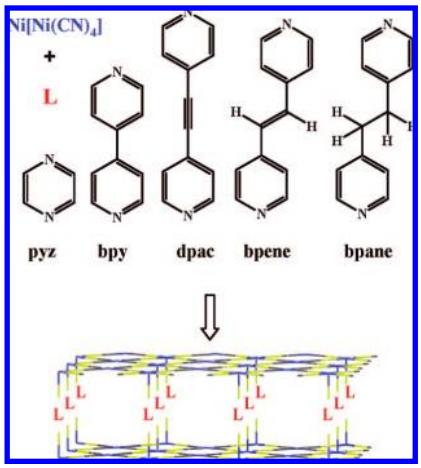

materials arises from the disruption of weaker hydrogen bonds or π-stacking interactions between the extended coordination networks. The weaker bonding interactions in these structures allow the microcavities to conform to the shape or functionality of the guest molecules when the host−guest interaction can energetically compensate for the accompanying loss of lattice energy. This thermodynamic requirement often results in a stepwise isotherm with some positive threshold pressure, after which substantial adsorption takes place. Subsequent desorption isotherms from the resulting host phase typically show a pronounced hysteresis.

Here we report a rare guest-induced structural transformation in an extended three-dimensional coordination polymer which is comprised of strong coordinate covalent bridges in all three dimensions. The unusual dynamic behavior is observed with solvent guests such as acetone and with weakly adsorbing guests such as CO_2 and N_2, the latter at temperatures above their respective critical points. The material described is a coordinate covalently bridged three-dimensional analogue of the well-known Hofmann clathrates. As shown in Scheme 1, the compound is formed by pillaring planar nickel cyanide networks with a quasi-linear bidentate ligand, 1,2-bis(4-pyridyl)ethylene (bpene). In the guest-free state the pillar ligands tilt away from the perpendicular, resulting in a condensed structure with low porosity. Upon exposure to acetone, CO_2, or N_2 above a threshold activity, the pillar ligands adopt a more perpendicular orientation with concomitant adsorption of the guest. The resulting adsorption isotherms show a distinct sigmoidal shape with increasing pressure. Subsequent desorption from the saturated state produces a large hysteresis, even when the temperature is well above the critical point for the respective gas. This unusual behavior is particular to the presence of the quasi-linear bpene linker. Other members of the homologus series that have the rigid linkers, pyrazine, 4,4′-bipyridine, or 4,4′-dipyridylacetylene, exhibit normal type I isotherms without evidence of hysteresis, as is typical of rigid microporous solids. When the linker is the more flexible 1,2-bis(4-pyridyl)ethane, however, the tilt of the pillars in the guest-free state is irreversible, and the collapsed material shows no uptake of CO_2. This dynamic host−guest interaction is very rare for an extended three-dimensional structure[4,14,19,20] and documents the potential for preparing functionalized porous materials with dynamic responses selectively tailored to specific guests.

Experimental Section

Synthesis. All chemicals were purchased from Sigma-Aldrich and used as received. The $Ni(H_2O)_2[Ni(CN)_4]\cdot 2H_2O$ compound was prepared by slowly mixing 0.1 M aqueous solutions of $K_2[Ni(CN)_4]$ and $Ni(NO_3)_2\cdot 6H_2O$ and refluxing the resulting mixture overnight. The product was subsequently filtered, washed well with water, and air-dried. Purity was verified by determination of NiO by thermogravimetric analysis (TGA) in dry air at 500 °C. Ni(pyrazine)[Ni(CN)$_4$] (NiPyzNiCN), Ni(4,4′-bipyridine)[Ni(CN)$_4$] (NiBpyNiCN), and Ni(1,2-bis(4-pyridyl)acetylene)[Ni(CN)$_4$] (NiDpacNiCN) were prepared as described peviously.[21] Ni(Bpene)[Ni(CN)$_4$] (bpene = 1,2-di(4-pyridyl)ethylene) and Ni(Bpane)[Ni(CN)$_4$] (bpane = 1,2-di(4-pyridyl)ethane) were prepared by modification of the previously reported procedure for the preparation of Ni(4,4′-bipyridine)[Ni(CN)$_4$].[21,22] Specifically, a 50 mL flask was charged with 2 mmol of $Ni(H_2O)_2[Ni(CN)_4]\cdot 3H_2O$ and the solid heated to 140 °C under a N_2 purge for 4 h. The sample was then cooled to room temperature, 2.1 mmol of bpene or bpane dissolved in 30 mL of acetone was added, and the mixture was refluxed for 2 days. The resulting solid was then filtered and washed well with acetone. The yields were quantitative. The X-ray diffraction (XRD) patterns were collected on freshly prepared materials; however, the materials lose acetone readily in air, and some desolvated phase is usually detectable in the XRD patterns. The purity of the samples was verified by determination of NiO by TGA in dry air at 500 °C. The structural integrity of the materials after the gas adsorption measurements was verified by powder XRD on the evacuated sample taken directly from the instrument, and after the sample was resolvated by soaking 1 h in acetone, and comparing the powder patterns to those of the as-synthesized materials.

Instrumentation. Isotherms were collected on a pressure-composition isotherm measurement system (Advanced Materials Corp.) for pressures up to ~80 bar for N_2 and ~20 bar for CO_2 over a temperature range of −78 to 40 °C. The instrument is designed on the basis of a conventional Sievert's apparatus. Prior to the measurements, samples (~750 mg) were degassed under vacuum at 85 °C overnight. Powder X-ray diffraction (PXRD) measurements were performed on a PANalytical X'Pert Pro MPD powder diffractometer having a Θ−Θ configuration, a Cu X-ray source operated at 45 kV and 40 mA, and an X'Celerator detector with a monochromator. Patterns were recorded over a 2Θ range of 5−50° using a step size of 0.02° 2Θ and a scan step time of 50 s per degree 2Θ. Thermogravimetric analyses were performed on ~5 mg samples using a Perkin-Elmer TGA7 thermogravimetric analyzer under a dry air purge of 20 mL/min. The samples were ramped to 500 °C at a rate of 5 °C/min.

Kinetics Experiments. The kinetic measurements for the desorption of acetone were made using a TEOM series 1500 pulse mass analyzer manufactured by Rupprecht and Patashnick (Albany, NY). This instrument was used in a similar study before.[23] Carrier gas passes through a small packed bed of sample at the end of a vibrating tapered glass element. Mass changes are detected by this inertial system by measuring changes in the vibrational frequency of the tapered element which nominally oscillates near 40 Hz. Samples (ca. 30 mg) were loaded and purged with dry argon, heated to expel all solvents from the synthesis, and charged with acetone vapor via a stream of argon saturated with acetone at 20 °C. After the mass stabilized, indicating saturation, the stream was switched to pure argon and the mass monitored as the acetone desorbed.

(19) Seki, K. *Phys. Chem. Chem. Phys.* **2002**, *4*, 1968.
(20) Zhang, J. P.; Kitagawa, S. *J. Am. Chem. Soc.* **2008**, *130*, 907.
(21) Culp, J. T.; Natesakhawat, S.; Smith, M.; Bittner, E.; Matranga, C.; Bockrath, B. *J. Phys. Chem. C* **2008**, *112*, 7079.
(22) Mathey, Y.; Mazieres, C.; Setton, R. *Inorg. Nucl. Chem. Lett.* **1977**, *13*, 1.
(23) Smith, M.; Culp, J. T.; Bittner, E.; Parker, B.; Li, J.; Bockrath, B. *Microporous Mesoporous Mater.* **2007**, *106*, 115.

The same procedure was followed while the sample was held at several temperatures.

Inspection of the rate data showed that the decay curves were better fit by a combination of two first-order processes rather than by the use of only one first-order decay process. In a manner described previously,[23] a least-squares fit of calculated mass to the experimental values at 5 s intervals was performed using Microsoft Excel Solver using the expression

$$\text{mass}(t) = B + a\,e^{-k_1 t} + b\,e^{-k_2 t}$$

where B corrects for the nonzero baseline, a and b are the masses accounted for by the separate desorptions 1 and 2, and k_1 and k_2 are the rate constants. Goodness of fit, as measured by Pearson R^2, was greater than 0.999. The activation energies for the two desorption processes were determined from Arhennius plots.

Results

X-ray Diffraction Studies. The preparation and H_2 adsorption isotherms for a series of Ni(L)[Ni(CN)$_4$] compounds, L = pyrazine, 4,4′-bipyridine, or 4,4-dipyridylacetylene, were recently reported.[21] The materials are layered solids with interlayer spacings of ~7, 11, and 14 Å, respectively. Complete structures for the materials have not been determined, but likely models based on powder diffraction data and the reported structure of Fe(pyrazine)[Pt(CN)$_4$] consist of two-dimensional sheets of Ni[Ni(CN)$_4$]$_n$ which are pillared by bridging of the octahedral nickel centers along the z-axis by (L).[24]

Following a procedure similar to that used for the preparation of Ni(L)[Ni(CN)$_4$] and substituting bpene or bpane for (L) gave homologous materials containing acetone guests with interlayer spacings of 13.6 and 12.5 Å, respectively. Unlike the previous series of rigid Ni(L)[Ni(CN)$_4$] compounds, with L = pyz, bpy, or dpac, which showed little structural variation as a function of guest loading, the interlayer spacing in the bpene and bpane pillared samples is sensitive to the amount of guests which are adsorbed and decreases to 12.2 and 9.0 Å, respectively, in their fully desolvated states. The PXRD patterns for both the guest-loaded and guest-free Ni(L)[Ni(CN)$_4$] materials for L = dpac, bpene, and bpane are shown in Figure. The XRD patterns show a variation in structural stability as a function of the flexibility of (L). For the rigid dpac pillared sample, the interlayer spacing indicated by the position of the (001) reflection remains essentially constant between the guest-loaded and guest-free phases, with only slight variations noticeable between the two respective diffraction patterns. As the pillar becomes more flexible in the bpene pillared material, a measurable structural transition appears with guest loss. This is shown by the increase in diffraction angle of the interlayer (001) reflection and equates to a 10% reduction in interlayer spacing. The phase transition is reversible, and either phase can be generated by adsorption or desorption of an appropriate guest. When the pillar ligand is replaced by an even more flexible bpane linker, losses of guests induce an irreversible 30% reduction of the interlayer spacing.

Gas Adsorption Measurements. The CO_2 adsorption isotherms for Ni(Bpene)[Ni(CN)$_4$] at several temperatures are shown in Figure 2. The isotherms at each temperature show a similar stepwise behavior beginning with a gradual gain in uptake with pressure until an adsorption of ~1 CO_2 per pore. Then uptake increases more rapidly with pressure toward a saturation adsorption of ~2.5 CO_2 per pore. A "pore" refers in this case to the equivalent of a total adsorption volume per

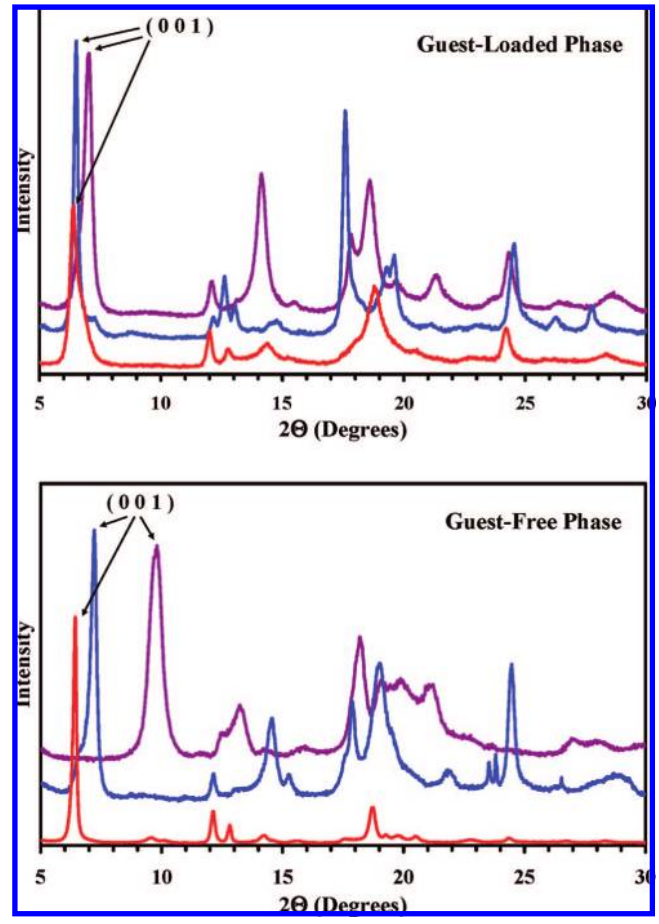

Figure 1. X-ray powder diffraction scans for Ni(L)[Ni(CN)$_4$] showing the variation in interlayer spacing (based on the (001) reflection) between the guest-loaded phases (upper plot) and the guest-free phases (bottom plot). As the pillar ligand (L) becomes more flexible, the interlayer spacing for the guest-free phase becomes more compressed. The rigid dpac pillared sample shows no significant compression when guests are removed, and the porosity is preserved. For the intermediate case when L = bpene, a small reversible compression occurs which allows for a dynamic adsorption behavior with guests such as CO_2, N_2, and acetone. The phase change in the extreme case when L = bpane is irreversible, with no re-adsorption of guests. Key: L = dpac, red; L = bpene (blue); L = bpane (violet).

Table 1. Inflection Point (IP) Conditions in the CO_2 Isotherms on NiBpeneNiCN

T, °C	P_{IP}, atm	Q_{IP} (no. CO_2/pore)
0	4.0	1.47
7	4.7	1.34
15	5.8	1.32
22	7.7	1.28
30	9.8	1.28
40	13.0	1.14

Ni(Bpene)[Ni(CN)$_4$] formula unit. As such, 1 CO_2 per pore is equivalent to 110 mg of CO_2/g of sorbent. The isotherms are symmetrical in the sense that the adsorption values at the inflection points of the isotherms occur at approximately half the saturation uptakes. As summarized in Table 1, the inflection points (determined from Gaussian fits to the slopes of the isotherms) shift to higher pressure and the coverage at the inflection point decreases slightly as the temperature of the sample is increased. This type of behavior is consistent with a physisorption process.

Reduction of the pressure after saturation of the sample results in the desorption hysteresis plotted in Figure 3. The hysteresis

(24) Niel, V.; Martinez-Agudo, J. M.; Munoz, M. C.; Gaspar, A. B.; Real, J. A. *Inorg. Chem.* **2001**, *40*, 3838.

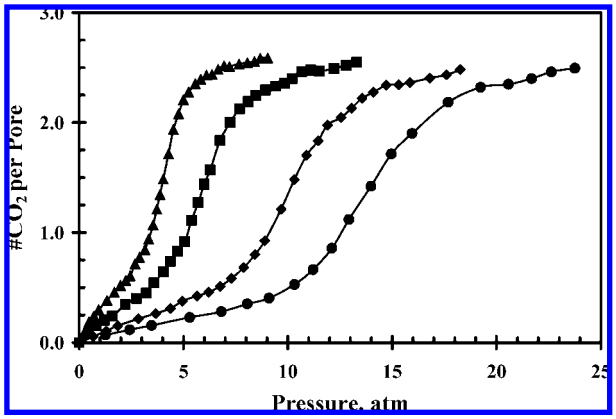

Figure 2. Adsorption isotherms for CO_2 on NiBpeneNiCN at several temperatures. From left to right, $T = 0$, 15, 30, and 40 °C. Lines are drawn as a guide to the eye. Note: 1 CO_2 per pore is equivalent to 110 mg of CO_2/g of sorbent.

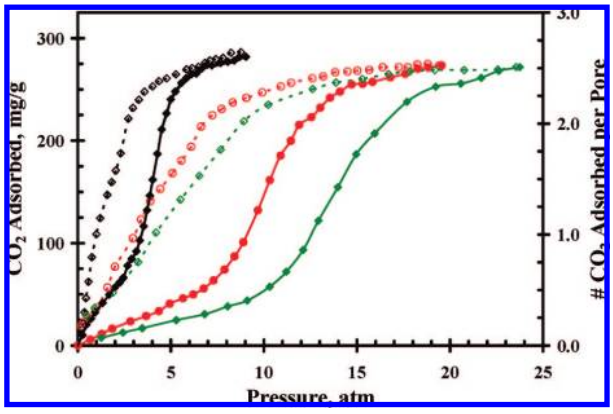

Figure 3. Hysteretic adsorption (solid) and desorption (open) cycles for CO_2 on NiBpeneNiCN at temperatures, from left to right, of 0, 30, and 40 °C. The solid lines (adsorption) and dashed lines (desorption) are given as a guide to the eye.

gets more pronounced at higher temperatures, as evident from the increased width of the hysteresis loops. At 40 °C, the desorption coverage drops by less than 10% at one-half the saturation pressure of the adsorption isotherm. Also of note is the nearly 5-fold increase in coverage at 10 atm between the desorption and corresponding adsorption uptake. The existence of such a pronounced hysteresis at a temperature above the critical temperature of CO_2 rules out a pore condensation mechanism and indicates that the phenomenon is the result of a structure transition.

The hysteretic adsorption behavior can also be demonstrated by a thermal process. The plot in Figure 4 shows how the CO_2 coverage changes under isobaric conditions as a function of temperature after first saturating the sample under 7 atm of CO_2 at 0 °C. Subsequent warming of the sample from 0 to 30 °C causes the amount of adsorbed CO_2 to drop from 275 to 200 mg/g. This drop in coverage with increasing temperature is consistent with a physisorption process; however, the final coverage obtained at 30 °C by this thermal process is more than double the 80 mg/g uptake measured at 7 atm in the 30 °C adsorption isotherm which started from an evacuated state (see also the data in Figure 3). In fact, this coverage is very close to the value measured at 7 atm in the 30 °C *desorption* isotherm which started from a saturated state (see also the data in Figure 3). Thus, the hysteretic behavior provides a means for achieving a much higher loading of CO_2 at lower relative pressures by

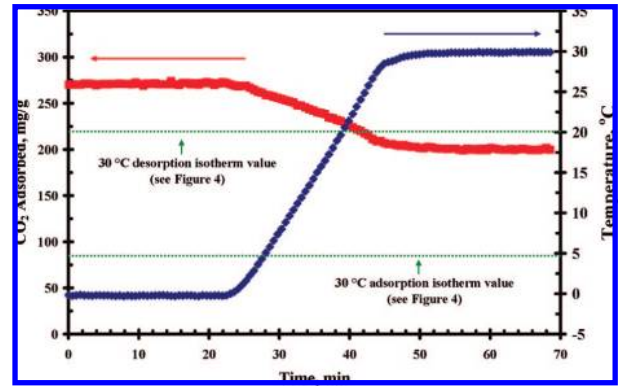

Figure 4. Change in coverage of CO_2 (red, left axis) on NiBpeneNiCN after saturation at 0 °C. As the sample temperature (blue, right axis) increases from 0 to 30 °C under an isobaric condition of 7 atm, the final coverage approaches the value obtained in the 30 °C desorption isotherm (upper dashed green line) and not the value in the 30 °C adsorption isotherm (lower dashed green line).

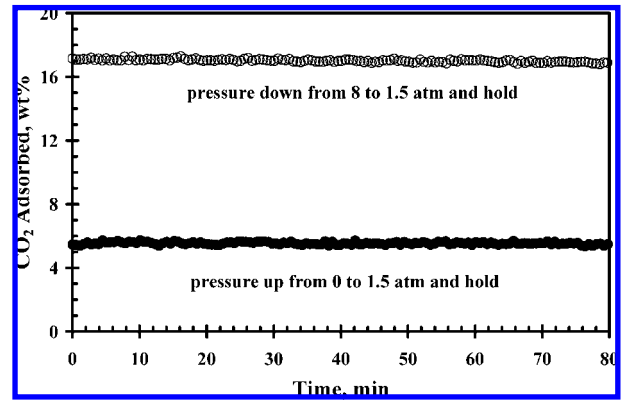

Figure 5. Stability of CO_2 coverage with time on NiBpeneNiCN. The upper points are after first saturating at 8 atm and then releasing the pressure to 1.5 atm and holding. The lower points are after pressurizing from an evacuated state to 1.5 atm and holding. Both measurements were taken at 0 °C.

first saturating the material at low temperature and then warming the material to room temperature.

In order to verify that the observed hysteresis was not the result of a slow approach to equilibrium, a series of experiments was conducted to investigate the stability of the coverage with time. The data in Figure 5 show the stability of the coverage with time at 0 °C in both the adsorption and desorption isotherms. The lower set of points plots the coverage obtained when pressurizing the sample from 0 to 1.5 atm and holding for 80 min, whereas the upper markers plot the coverage obtained when dropping from the saturation coverage at 8 atm down to 1.5 atm and holding for 80 min. Neither data set shows any significant change in coverage with time, indicating pseudo-equilibrium has been achieved on both the adsorption and desorption legs that persists for a very long time.

The hysteretic adsorption is not reversible in the sense that the ensuing adsorption isotherm does not retrace the previous desorption isotherm. The plot in Figure 6 shows the result at 0 °C when an adsorption run is started from a point in the preceding desorption isotherm. The lower solid blue line shows the initial adsorption isotherm taken to saturation. As the pressure is dropped to 0.7 atm, the coverage follows the dashed blue line. If the adsorption isotherm is then restarted from this point, the curve does not follow the desorption curve but instead

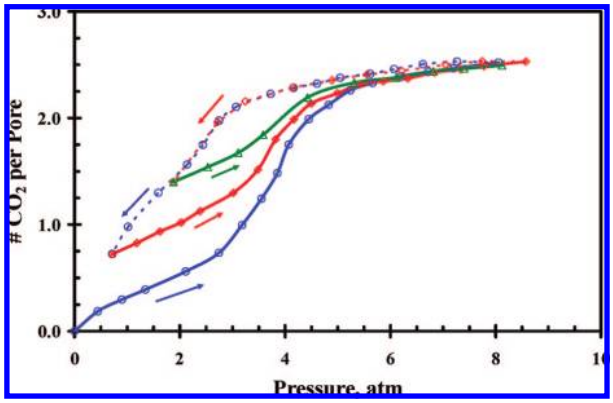

Figure 6. Adsorption (solid)/desorption (dashed) cycles for CO_2 on NiBpeneNiCN at 0 °C. The initial pressurization is shown in the solid blue, with the subsequent partial depressurization in the dashed blue line. A second pressurization immediately follows, shown in the solid red trace, followed by the partial depressurization in the dashed red line. A third pressurization then follows, shown in the solid green trace.

follows the intermediate stepwise isotherm shown as the solid red trace. If the sample is taken again to saturation and dropped to a pressure of 1.9 atm (dashed red trace), the following adsorption isotherm shown by the solid green trace again follows an intermediate path with a noticeable inflection point.

The sigmoidal nature of the isotherms makes it difficult to get accurate calculations of the heats of adsorption by the usual method of comparing isotherms at different temperatures using curves fit by an adsorption model such as the Langmuir−Freundlich equation. However, the heat of CO_2 adsorption was estimated by intercalation of the data points and application of these values to the Clausius−Clapeyron equation. The heats of adsorption remain relatively consistent at 25 ± 3 kJ/mol for both the adsorption and desorption isotherms. These data are included in the Supporting Information.

Attempts were made to measure the N_2 BET surface area and pore volume of the material by the usual method of N_2 adsorption at 77 K. However, no significant adsorption of N_2 was observed at 77 K and 1 atm of pressure. High-pressure isotherms up to 80 atm for N_2 in the temperature range of −40 to −78 °C did show significant uptakes, with isotherm profiles very similar to those observed for CO_2. The N_2 adsorption/desorption isotherms at −78 °C are given in Figure 7. An even more pronounced hysteresis is observed in the desorption isotherm, with 90% of the saturation coverage remaining at less that one-third the adsorption saturation pressure. We note in particular that, in this case, the desorption branch does not rejoin the adsorption branch until very close to the origin. Again, this pronounced hysteresis is observed for a gas at a temperature well beyond its critical temperature of 126.2 K.

Acetone Adsorption Experiments. Adsorption experiments with acetone were conducted in order to determine the mechanism of the hysteretic behavior. The adsorption was measured with a pulsed mass analyzer by exposing the sample to various partial pressures of acetone in argon that served as a carrier gas. The acetone pressure was controlled by blending pure argon with argon saturated with acetone at room temperature via mass flow controllers. The adsorption isotherm as a function of acetone partial pressure was then constructed. The adsorption/desorption cycle of acetone followed a similar hysteretic behavior at 120 °C (see Supporting Information).

Due to the higher heat of adsorption, the kinetics of desorption were slow enough to measure experimentally by simply loading the sample with acetone and then cutting the flow to pure argon and measuring the mass loss in the sample over time. The best fits to the mass decay curves were obtained by a linear addition of two separate exponential decay functions (see Supporting Information). Two separate rate constants were extracted from these fits, and the results are listed in Table 2. The desorption process occurred at two different rates when more than one acetone was adsorbed in a pore site. For example, at 70 °C, after the partial pressure of acetone was rapidly cut to zero, the first guest desorbed with a rate constant of 3.67×10^{-3} s^{-1}, which corresponds to a half-life of 189 s, while the second guest desorbed more slowly, with a rate constant of 4.77×10^{-4} s^{-1} and a half-life of 1450 s. The activation energy for these two processes was calculated by the Arrhenius equation to be 55 and 68 kJ/mol, respectively.

Table 2. Kinetics Data for the Desorption of Acetone off NiBpeneNiCN[a]

	T, °C			
	70	80	90	100
k_1 (s^{-1})	3.67×10^{-3}	6.24×10^{-3}	9.56×10^{-3}	1.71×10^{-2}
k_2 (s^{-1})	4.77×10^{-4}	9.33×10^{-4}	1.54×10^{-3}	3.03×10^{-3}
$t_{1/2}$-1 (s)	189	111	72.5	40.4
$t_{1/2}$-2 (s)	1450	743	451	229

[a] For loadings greater than one acetone per pore, k_2 and $t_{1/2}$-2 reflect the rate constant and half-life for the desorption of 1 equiv of acetone, and k_1 and $t_{1/2}$-1 reflect the rate constant and half-life for the desorption of acetone in excess of 1 equiv.

Discussion

Step-shaped and hysteretic adsorption isotherms have long been studied in lamellar clays.[25−27] More recently, the phenomenon has been associated with a new generation of flexible MOFs. In both classes of extended inorganic materials, these adsorption behaviors have been correlated with structural phase changes that result from the adsorption of guests into initially closed or confined structures. These guests can be small solvent molecules such as water, alcohols, acetone, or small aromatics, but in rare cases even the adsorption of weaker interacting light gases such as CO_2, O_2, CH_4, and N_2 can induce a structural change.[3,4,13,19,20,28−32] The structural phase changes in these systems are usually made possible by the presence of weaker π-stacking or hydrogen-bonding interactions within the host lattices and most often occur between one- or two-dimensional extended coordination polymers within the host crystal.

Flexible systems which are linked in three dimensions through coordinate covalent bonds are rarer since these bonding interactions are typically more rigid and more thermodynamically stable.[4,14,19,20] Flexibility in the extended structures can be introduced through interligand interactions. One example of such a system is the pillared layered solid $[Cu_2(pzdc)_2(dpyg)]_n$ (pzdc

(25) Barrer, R. M. *Philos. Trans. R. Soc. London A: Math. Phys. Eng. Sci.* **1984**, *311*, 333.
(26) Barrer, R. M. *Pure Appl. Chem.* **1989**, *61*, 1903.
(27) Burgess, C. G. V.; Everett, D. H.; Nuttall, S. *Pure Appl. Chem.* **1989**, *61*, 1845.
(28) Goto, M.; Furukawa, M.; Miyamoto, J.; Kanoh, H.; Kaneko, K. *Langmuir* **2007**, *23*, 5264.
(29) Kaneko, K.; Murata, K. *Adsorption−J. Int. Ads. Soc.* **1997**, *3*, 197.
(30) Kitaura, R.; Seki, K.; Akiyama, G.; Kitagawa, S. *Angew. Chem., Int. Ed.* **2003**, *42*, 428.
(31) Noguchi, H.; Kondoh, A.; Hattori, Y.; Kanoh, H.; Kajiro, H.; Kaneko, K. *J. Phys. Chem. B* **2005**, *109*, 13851.
(32) Zhao, X. B.; Xiao, B.; Fletcher, A. J.; Thomas, K. M.; Bradshaw, D.; Rosseinsky, M. J. *Science* **2004**, *306*, 1012.

Scheme 2. Proposed Mechanism for Guest-Induced Phase Transition in Ni(Bpene)[Ni(CN)$_4$][a]

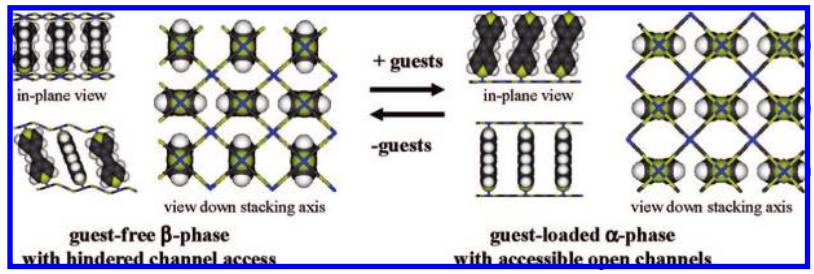

[a] Based on qualitative structural models for the two phases observed for the material. The mechanism shows how a transition from a compressed tilted arrangement of pillar ligands in the guest-free β-phase to a more vertical alignment in the guest-loaded α-phase can create channels for guest adsorption.

= pyrazine-2,3-dicarboxylate; dpyg = 1,2-di(4-pyridyl)glycol) reported by Kitaura et al., which showed a structural phase change upon exposure to methanol and a subsequent hysteretic adsorption/desorption cycle.[14] The structural change results from the disruption by methanol of the interpillar hydrogen bonds. A similar effect is observed in the current study of NiBpeneNiCN, which is also a pillared layered solid. The main difference between the two is the nature of the interligand interactions. In NiBpeneNiCN, the interligand distances are large for $\pi-\pi$ interactions. This loose packing arrangement produces weak intermolecular forces that are more easily overcome by lower energy guests such as CO_2 or N_2.

Results from the diffraction and isotherm experiments are consistent with the view that the adsorption of guests such as CO_2, N_2, and acetone overcomes the tilt of the bpene ligands above the onset pressure and force the adoption of a more perpendicular arrangement of the ligands with respect to the Ni[Ni(CN)$_4$]$_n$ sheet. This phase transition is clearly evidenced by the larger interlayer spacing measured in the guest-loaded material. Complete structural analyses for the two phases are not possible due to the quality of the XRD patterns resulting from the small particle sizes, but some qualitative conclusions can be derived. It is well-known that layered motifs are favored in coordination polymers incorporating d^8 tetracyano complexes. Layered structures are predominant in the widely studied 2-D Hofmann clathrates and in the pillared 3-D analogues such as Fe(pyrazine)[Pt(CN)$_4$] and the series of α,ω-diaminoalkane cadmium tetracyanonickelates.[24,33] Using these pillared materials as models by keeping the a and b dimensions consistent with the typical dimensions of the planar M[Ni(CN)$_4$] network and using a typical length for the bpene ligand as the interlayer c dimension, a unit cell of a = 7.3 Å, b = 7.0 Å, c = 13.6 Å, and β = 97° can be qualitatively assigned to the guest-loaded phase of NiBpeneNiCN. The β angle of 97° reflects the offset of the two pyridyl nitrogens in the bpene linker. The calculated Miller indices for the model cell in the absence of any symmetry or space group assignments agree well with the observed powder diffraction pattern (see Supporting Information). Continuing this approach for the guest-free phase, a shorter interlayer spacing of 12.2 Å can be accounted for by simply increasing the β angle of the unit cell which would result from a larger tilt angle of the bpene pillar. Such rhombic distortions are common in the stacking alignment of layered M(L)$_x$Ni(CN)$_4$ coordination polymers and result from a puckering of the M[Ni(CN)$_4$] network.[33,34] While the increased tilt angle accounted for the compression of the interlayer spacing, the best match to the peak positions in the powder diffraction pattern for the guest-free phase was obtained by using a unit cell of a = 14.6 Å, b = 7.3 Å, c = 13.3 Å, and β = 114°. Using this unit cell, a qualitative structural model was created with an alternating packing arrangement of the pillar ligands as shown in Scheme 2. (A comparison of the observed peak positions and those calculated for the model unit cell is given in the Supporting Information.) While a full structural refinement is not possible due to the quality of the powder diffraction data, the qualitative structural models do provide a hypothetical mechanism, shown in Scheme 2, for the unusual adsorption behavior observed for the two NiBpeneNiCN phases. The more perpendicular arrangement of the bpene ligand in the guest-loaded phase would allow freer rotation about the ligand axis, giving rise to the open channel structure shown in Scheme 2, α-phase. When the tilt angle is increased in the guest-free phase, the bpene−bpene separation is reduced. The resulting reduction in interligand separation could either hinder the rotational freedom of the pillar ligands and prevent the open channel alignment needed for guest adsorption from forming or simply block access to the pore sites by a gating effect mediated by the narrow interligand gaps (Scheme 2, β-phase). Such a rotational barrier could also explain the lack of any significant adsorption of N_2 at 77 K up to 1 atm of pressure in attempts to measure the BET surface area of the NiBpeneNiCN sample, whereas a significant uptake of N_2 is observed at 195 K and 50 atm pressure.

Further insight into the mechanism for the guest-induced phase transition can be gained by analyzing the CO_2 adsorption/desorption isotherms for several Ni(L)[Ni(CN)$_4$] analogues where L is one of the rigid pillar ligands pyrazine (pyz), 4,4′-bipyridine (bpy), or dipyridylacetylene (dpac). Powder XRD measurements on these rigid analogues verified the absence of any significant change in interlayer spacing as a function of guest solvent loading. Consequently, their CO_2 isotherms show the usual type I behavior without any steps or adsorption/desorption hysteresis (see Supporting Information). It is particularly useful to compare the isotherm behaviors of the dpac and bpene pillared materials since the molecular dimensions of dpac and bpene are very similar. In the guest-loaded state, the interlayer spacing in the NiDpacNiCN sample is 13.7 Å versus 13.6 Å in the NiBpeneNiCN sample. In the guest-free state, the NiDpacNiCN sample interlayer spacing is practically unchanged, whereas the NiBpeneNiCN sample interlayer spacing drops to 12.2 Å. As indicated in the CO_2 isotherms shown in Figure 8 for the two samples, the NiBpeneNiCN sample ultimately shows the same CO_2 capacity as the NiDpacNiCN sample after the step in the isotherm is completed. This equality in CO_2 capacity between the NiDpacNiCN and NiBpeneNiCN

(33) Nishikiori, S. I.; Hasegawa, T.; Iwamoto, T. *J. Inclusion Phenom. Mol. Recognit. Chem.* **1991**, *11*, 137.
(34) Niu, T. Y.; Crisci, G.; Lu, J.; Jacobson, A. J. *Acta Crystallogr., C: Cryst. Struct. Commun.* **1998**, *54*, 565.

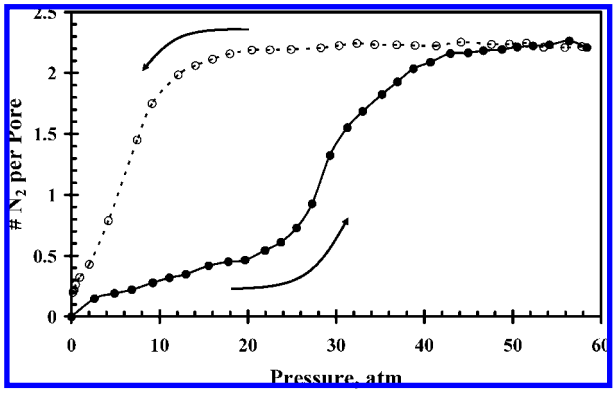

Figure 7. Adsorption (solid)/desorption (open) cycle for N_2 on NiBpeneNiCN at −78 °C.

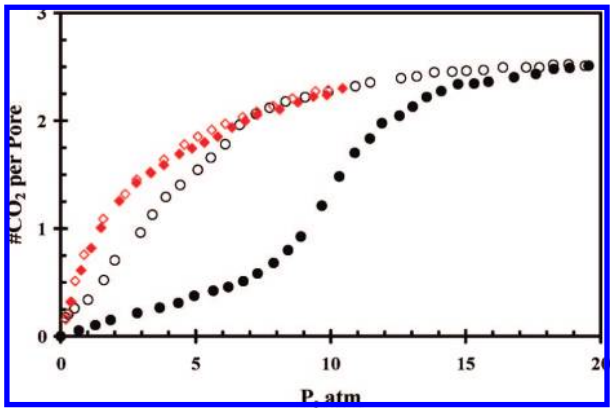

Figure 8. Plot highlighting the different isotherm behaviors at 30 °C for CO_2 on Ni(Bpene)[$Ni(CN)_4$] (black circles) and Ni(Dpac)[$Ni(CN)_4$] (red diamonds). Adsorption data are solid symbols, and desorption data are open symbols.

samples provides convincing evidence that the two materials have reached a similar structural phase in the saturated state. As the CO_2 pressure is dropped, the desorption isotherm for the NiBpeneNiCN sample initially follows a trace similar to that of the NiDpacNiCN sample but then deviates at lower pressure as CO_2 is lost more readily. This deviation in the NiBpeneNiCN isotherms is inline with the proposed structural phase transition to a more collapsed structure in the evacuated state.

The guest-free collapsed state is clearly evident in the bpane pillared sample. The PXRD measurements displayed in Figure 1 show a pronounced structural transition as the guest solvents are removed. The decrease in interlayer spacing is approximately 3 times the magnitude of that observed in the bpene sample. Using the same approach as described above for NiBpeneNiCN, unit cells for NiBpaneNiCN were determined for both the guest-loaded and guest-free materials as $a = 6.9$ Å, $b = 7.3$ Å, $c = 12.7$ Å, $\beta = 97$ and $a = 7.0$ Å, $b = 7.1$ Å, $c = 10.2$ Å, $\beta = 119$, respectively (see Supporting Information). The increased compression of the interlayer spacing in the guest-free bpane sample renders the phase transition irreversible, and the sample shows no CO_2 uptake even at −23 °C and 10 atm.

Thus, the bpene material can exhibit properties of either rod-like pyz, bpy, and dpac materials or the more flexible bpane pillar material depending on the environmental conditions. This dynamic property is derived from a combination of the molecular geometry and the conjugated bonding system of the ligand. Unlike the pyz, bpy, and dpa which are strict linear linkers, the diaza bonding sites in bpene are offset one from another by ∼7° due to the ethylene bridge between the two pyridine moieties. This slight offset changes the packing arrangement of the pillars in relation to the rigid linear linkers. Furthermore, the conjugated bonding of the bpene ethylene linker reduces the flexibility of the ligand in relation to the ethane linker in bpane and prevents the material from irreversibly collapsing into a close-packed nonporous state. The most arresting property of NiBpeneNiCN is the pronouced hysteresis in the desorption isotherm. Such a hysteresis can be the result of kinetic effects due to small pore sizes or steric effects which hinder the desorption process. In NiBpeneNiCN, a kinetic mechanism can be ruled out, as shown by the data in Figure 5. The adsorption and desorption values remain constant with time, indicating that the acquired metastable state is in equilibrium. The increase in coverage obtained when reaching the same relative sample pressure from a higher pressure state versus a lower pressure state is the result of the structural phase change in the adsorbent. In essence, when loading the sample from an initial evacuated state, the isotherm is measured on a low-porosity, condensed β-phase which results from a highly tilted arrangement of the pillar ligands (see Scheme 2). As the activity of the guest is increased, eventually the adsorption energy overcomes a barrier necessary for a structural phase change, the ligand tilt is reduced, and a more open structure obtained. The subsequent desorption isotherm is then measured on the higher porosity, less condensed α-phase.

The propagation of the structural phase change and its effect on the adsorption behavior can be gathered from the results shown in Figure 6. The adsorption isotherm was restarted after partial desorption of the CO_2. The resulting isotherms (solid red and green traces) show inflections similar to those observed in the original adsorption isotherm (solid blue trace), even though the subsequent isotherms are starting from coverages corresponding to the inflection onset of the original adsorption curve. Such a behavior shows that the desorption process does not occur in a stepwise fashion wherein one guest remains to "prop open" the structure and thereby facilitate the desorption/adsorption of the excess guests. Instead, a fraction of the material is losing all guests and collapsing back to the initial guest-free α-phase which then, upon pressurizing, goes again through the structural phase change with the associated step in the isotherm. Further evidence for this mechanism is obtained from the acetone kinetics experiments. Fits to the desorption curves gave the two rate constants listed in Table 2, indicating that, when more than one guest is adsorbed, the two desorb at different rates. Thus, in the desorption isotherm, the two adsorbed guests have to overcome two different activation barriers. The first guest is lost more easily, the second more slowly. The result is that there is always some of the material that becomes guest-free as the pressure drops, preventing the desorption leg from being reversible in the hysteretic desorption/adsorption cycle.

Interpretation of the thermodynamics involved in adsorption processes involving flexible MOFs is not as straightforward as in rigid porous systems.[12,35,36] Stepped adsorption isotherms and adsorption/desorption hysteresis cycles have been widely studied in lamellar clays, and the qualitative interpretation of the phenomena and the conditions needed for these behaviors given by Barrer can readily be extended to flexible MOFs.[26] In

(35) Uemura, K.; Kitagawa, S.; Saito, K.; Fukui, K.; Matsumoto, K. *J. Therm. Anal. Calorim.* **2005**, *81*, 529.
(36) Uemura, K.; Saito, K.; Kitagawa, S.; Kita, H. *J. Am. Chem. Soc.* **2006**, *128*, 16122.

essence, the change in free energy of the system, ΔG_{sys}, is the sum of the free energy change which results from the structural phase transition, ΔG_{phase}, and the free energy change accompanying the adsorption of the guests, ΔG_{ads}. The resulting free energy relationship can be summarized by eq 1.

$$\Delta G_{sys} = \Delta G_{ads} + \Delta G_{phase} + \Delta G_{\sigma} + \Delta G_{s} \quad (1)$$

The ΔG_{phase} is always a positive term reflecting the energy required to transition the structure from the guest-free phase to the intercalated phase, whereas the ΔG_{ads} term is a negative quantity due to the exergonic adsorption of the guest. The onset in the adsorption isotherm thus occurs at a temperature and pressure where the magnitude of ΔG_{ads} is equal to the magnitude of ΔG_{phase}. This onset is further modified by the energy costs associated with the lattice strain, ΔG_s, and interfacial free energy, ΔG_{σ}, accompanying the growth of the new domain which effectively delays the intercalation to pressures above the true equilibrium threshold pressure. The reverse of this domain growth process works to lower the threshold pressure in the desorption part of the cycle. The cumulative effects of these energy requirements are the stepped adsorption isotherm and hysteretic desorption isotherm observed in the NiBpeneNiCN material.

It is also interesting to relate the sigmoidal isotherms observed for the NiBpeneNiCN material to the recent report of similar sigmoidal CO_2 adsorption isotherms in larger pore, rigid MOFs.[37] The sigmoidal isotherms in the rigid MOFs could be accurately modeled by taking into account CO_2-CO_2 electrostatic interactions without the need to invoke crystal transformations. While the electrostatic model is very effective at reproducing the sigmoidal isotherms in the rigid MOFs, such a mechanism alone cannot explain the isotherms observed with the current NiBpeneNiCN material, since the same isotherm shape and large hysteresis are observed for acetone and N_2, a molecule for which electrostatic interactions would not be expected to contribute significantly. Further evidence that a separate mechanism is responsible for the adsorption behavior of NiBpeneNiCN can be gathered from the data shown in Figure 6. Whereas electrostatic interactions would be expected to contribute above a threshold concentration of CO_2 when CO_2-CO_2 contacts become significant, the inflection points in the isotherms shown in Figure 6 indicate that the isotherm inflection point is determined instead by a domain growth process where the inflection point in the adsorption isotherm is determined by the starting concentration of CO_2 in the material and thus the number of domains which have already undergone a phase transition. These observations, combined with the noted phase changes seen in the powder diffraction data, clearly indicate that the dynamic behavior of the host is the main contribution to the sigmoidal shape of the adsorption isotherms and strong hysteresis in the desorption isotherms.

Conclusion

A three-dimensional pillared Ni(Bpene)[$Ni(CN)_4$], structurally related to the well-know Hofmann clathrates, has been prepared by the insertion of 1,2-di(4-pyridyl)ethylene bridging ligands between the $Ni[Ni(CN)_4]_n$ sheets. The linear bidentate bpene ligand bridges the $Ni[Ni(CN)_4]_n$ sheets by coordination to the available axial sites on the octahedral Ni centers located within the $Ni[Ni(CN)_4]_n$ planes. The resulting solid is a variable three-dimensional compound which shows dynamic behavior in the presence of guests such as acetone, N_2, and CO_2. In the fully evacuated state, the material compacts to a low-porosity structure through a tilting of the bpene bridging ligands. The material in this β-phase shows no significant uptake of N_2 at 77 K in a typical BET measurement. However, at -78 °C and elevated pressures, the compound adsorbs 2 equiv of N_2 per formula unit in a stepwise adsorption process. A similar stepwise isotherm is obtained for CO_2 at $0 < T < 40$ °C over moderate pressures of 7−20 atm. The sigmoidal shape of the isotherm can be attributed to a structural phase change wherein the tilt of the bpene ligands is reduced and a more open structure results. The resulting increase in pore volume allows for a 5-fold increase in guest uptake. Furthermore, the persistence of this structural phase results in a large adsorption hysteresis when the sample pressure is reduced. While other materials have been reported to show hysteretic adsorption of light solvents, NiBpeneNiCN is a much more unusual example of a covalently bridged three-dimensional coordination polymer which shows such hysteresis with weakly adsorbing guests such as N_2 and CO_2 at temperatures above their critical temperatures. The ability of such weakly adsorbing guests to introduce structural phase changes may provide a means for tailoring flexible materials with narrow pore apertures that could give enhanced separation behaviors or increased storage at lower partial pressures.

Acknowledgment. This technical effort was performed in support of the National Energy Technology Laboratory's ongoing research in CO_2 capture under the RDS contract DE-AC26-04NT41817. M.R.S. and E.B. were supported through an Oak Ridge Institute for Scientific Education (ORISE) Faculty Research Appointment at NETL. The authors thank Elizabeth Frommell at NETL for her assistance with the powder X-ray diffraction measurements and Sheila Hedges at NETL for her assistance with the TGA measurements. Reference in this work to any specific commercial product is to facilitate understanding and does not necessarily imply endorsement by the United States Department of Energy.

Supporting Information Available: Acetone adsorption/desorption isotherm for NiBpeneNiCN, kinetics data for acetone desorption from NiBpeneNiCN, CO_2 adsorption/desorption isotherms for $Ni(L)[Ni(CN)_4]$ compounds, heats of adsorption for CO_2 on $Ni(L)[Ni(CN)_4]$ compounds, model unit cells for both phases of NiBpeneNiCN, and calculated XRD line positions for NiBpeneNiCN and NiBpaneNiCN. This material is available free of charge via the Internet at http://pubs.acs.org.

JA802474B

(37) Walton, K. S.; Millward, A. R.; Dubbeldam, D.; Frost, H.; Low, J. J.; Yaghi, O. M.; Snurr, R. Q. *J. Am. Chem. Soc.* **2008**, *130*, 406.